

Liquid Halides: Structure, Pair Potentials, Energy and Ion Charges

D. K. Belashchenko* and O. I. Ostrovski

**Department of Physical Chemistry, Moscow Steel and Alloys Institute,
4 Leninskij Prospekt, Moscow, 119049 Russian Federation
School of Materials Science and Engineering, University of New South Wales,
Sydney, 2052 Australia*

(Received November 28, 2003; final form December 10, 2003)

ABSTRACT

This paper presents results of computer modelling of molten halides of alkali, alkaline-earth and noble metals and calculation of their structural and thermodynamic characteristics, pair potentials and ionic charges. Pair potentials were established using algorithm BELION, in which a non-Coulomb part of interaction potential was determined by the method of iterative simulation, which targeted agreement between calculated and experimental partial pair correlation functions. The models were constructed by molecular dynamics simulation. The ionic charges in salts, which can be fractional, were determined by minimisation of internal energy. Charges of rubidium and caesium in chlorides were found to be 1.10 and 1.22 respectively, while lithium and sodium in chlorides had a charge close to 1.0. Charges of Cu and Ag in liquid halides were in the range of 1.15-1.48. The charge of alkaline-earth metals in liquid halides was in the range of 2.0-2.1, slightly increasing from Mg to Ba.

1. INTRODUCTION

Halides have predominately ionic bonds, which makes them a relatively easy subject for theoretical consideration. A structure of molten halides was intensively studied by diffraction analysis [1, 2], in which partial structure factors and pair correlation functions for a number of systems were established.

This gives an impetus to further development of computer modelling of halides.

Molecular dynamics models for a number of molten halides were constructed with simple interaction potentials, which include Coulomb interaction, ionic core repulsion, dipole-dipole and dipole-quadruple interactions [2]. The use of these potentials with Fumi-Tosi parameters [3] gave good results for alkali halides. However, it was impossible to reproduce accurately enough structure of halides of alkaline-earth and noble metals.

Recently, Omote *et al.* [4] and Waseda *et al.* [5] developed an iterative method of calculation of effective ionic potentials in molten salts on the basis of the hypernetted chain approximation. It was applied for liquid NaCl [4,5], CuBr [5,6], AgBr, CuBr, CuI и RbBr [7]. Calculated potentials for NaCl were in good agreement with "theoretical" potentials of Fumi-Tosi [3]. Monte-Carlo modelling of NaCl system reproduced well original experimental data, although for the CuBr system agreement was not so good.

A key factor in the computer modelling of ionic systems is an ionic charge and non-Coulomb part of the interaction potential. Usually, charges of alkali, noble and alkaline-earth metals in molten halides are assumed to be integers: 1 for alkalis and noble metals, and 2 for alkaline-earth metals. However, in reality, charges of metals in halides can be fractional, which can have a strong effect on the structure and properties of the models. The ionic charge can be calculated using quantum mechanics technique [8] or found empirically

as an adjusting parameter to match calculated structural and/or thermodynamic characteristics to experimental data /9/. In this paper, the ionic charges in molten halides are found by minimisation of internal energy. This provides good agreement of the models' structure and thermodynamic properties with experimental characteristics.

An iterative algorithm, BELION, was suggested for modelling of ionic melts on the basis of diffraction data /10/. This algorithm is similar to a two-component Schommers algorithm /11/ which was successfully used for modelling of liquids with short-range potentials (for example, liquid metals) /12/. In the BELION algorithm, the ionic i - j potential is presented as:

$$u_{ij}(r) = \frac{Z_i Z_j e^2}{r} + \varphi_{ij}(r) \quad (1)$$

where Z_i is a charge of i -th ion, r is a distance between ions i and j , $\varphi_{ij}(r)$ is a short-range (non-Coulomb) part of a potential. Namely $\varphi_{ij}(r)$ is determined using diffraction data. If the partial pair correlation function (PPCF), determined experimentally, is $g^0_{ij}(r)$ and the calculated PPCF is $g_{ij}(r)$, then the relationship between $\varphi'_{ij}(r)$ (new approximation) and $\varphi_{ij}(r)$ (previous approximation) pair potentials can be presented in the form, which is analogous to the Schommers algorithm:

$$\varphi'_{ij}(r) = \varphi_{ij}(r) + kT^* \ln \frac{g_{ij}(r)}{g^0_{ij}(r)} \quad (2)$$

T^* in this equation is an effective temperature (generally tenths of the model's temperature) adjusted to provide the appropriate asymptotic behaviour of solution.

Algorithm BELION was used to model liquid NaCl, FeO, CuBr /10/, RbBr, CuCl, CuI, AgBr /13,14/, and ZnCl₂ /15/. This paper presents results of modelling and analysis of liquid halides of alkali, noble and alkaline-earth metals.

2. MODELLING OF LIQUID HALIDES

The structure of liquid halides was experimentally studied by the method of neutron diffraction with

isotope contrast /16/. Partial pair correlation functions were determined by Fourier transformation of experimental structure factors obtained *in-situ* at elevated temperatures. The error in measurement of PPCFs is difficult to estimate. Waseda and Toguri /17/ assessed the error in measurement of a distance between closest neighbours 0.001 nm, and the error in measurement of coordination number calculated from PPCFs of 0.2. An accuracy of PPCFs can be assessed by the Reverse Monte-Carlo (RMC) method, using a discrepancy parameter R_g , defined below (equation (3)).

The algorithm BELION developed in /10/ uses the molecular dynamics (MD) method. Coulomb potential is calculated in the Ewald-Hansen approximation with periodic boundary conditions. Non-Coulomb part $\varphi_{ij}(r)$ is adjusted in such a way to provide agreement between calculated and diffraction PPCF histograms. The agreement is achieved when the discrepancy parameter R_g , defined by equation (3) is of order 10^{-2} .

$$R_g = \left\{ \frac{1}{n_2 - n_1 + 1} \sum_{n_1}^{n_2} / g^0(r_i) - g(r_i) /^2 \right\}^{1/2} \quad (3)$$

In equation (3) n is a number of the histogram's elements. When a discrepancy parameter R_g is ~ 0.01 , $g^0(r)$ and $g(r)$ are practically indistinguishable.

MD models with a fixed number of ions in the basic cube were constructed at constant temperature and volume (NVT ensemble) /13/. The length of the basic cube edge at given temperature was calculated from the salt density. The Verlet algorithm was used to calculate particle positions at each step of the simulation. Each iteration of the algorithm BELION included 1000 steps with a time increment of 8.144×10^{-16} s.

3. CALCULATION OF ATOMISATION ENERGY AND IONIC CHARGE

Using the Ewald-Hansen method the Coulomb energy of the system is calculated with respect to isolated ions. To find atomisation energy, which is defined as the energy of transformation of a substance into isolated neutral atoms, the metals' ionisation potentials and non-metals' electron affinity should be

added to the energy calculated with respect to isolated ions.

The metal and non-metal charges $\pm Z$ can be fractional. In work [10], ionisation potentials and electron affinity energies were presented as functions of Z in the polynomial form. The following relationships were established for ionisation (cumulative) potentials of alkali metals, Cu and Ag, which accurately describe experimental data for $Z=+1$ and $+2$:

$$\begin{aligned} E(\text{Li}) &= Z(3.05084 + 2.34094 Z^4) \\ E(\text{Rb}) &= Z(0.2800 + 3.8970 Z^3) \\ E(\text{Cs}) &= Z(3.18710 + 0.70687 Z^4) \\ E(\text{Cu}) &= Z(1.441 + 6.283 Z) \\ E(\text{Ag}) &= Z(0.620 + 6.956 Z) \text{ eV} \end{aligned} \quad (4)$$

Ionisation potentials for alkaline-earth metals and zinc for charges in the range between $+1$ and $+3$ are represented by the following equations (eV):

$$\begin{aligned} E(\text{Mg}) &= Z(6.91187 + 0.121715 Z - 6.03214 Z^2) \\ E(\text{Ca}) &= Z(5.37172 + 0.15175 Z - 4.88538 Z^2) \\ E(\text{Sr}) &= Z(4.90991 + 0.178131 Z - 4.40235 Z^2) \\ E(\text{Ba}) &= Z(4.43554 + 0.189764 Z - 4.08857 Z^2) \\ E(\text{Zn}) &= Z(9.495 - 2.2985 Z + 2.1945 Z^2) \end{aligned} \quad (5)$$

These equations accurately reproduce ionisation potentials for $Z=+1$, $+2$ and $+3$.

Electron affinities for Br, Cl and I were presented as follows:

$$\begin{aligned} E_e(\text{Cl}) &= -Z(4.614 + 1.0 Z^3) \\ E_e(\text{Br}) &= -Z(4.34 + 0.8 Z^3) \\ E_e(\text{I}) &= -Z(3.78 + 0.7 Z^3) \text{ eV} \end{aligned} \quad (6)$$

Formulas (6) predict correctly the electron affinity for Cl^- , Br^- and I^- . The predicted electron affinity for $Z=2$ in the sequence $\text{Cl} \rightarrow \text{Br} \rightarrow \text{I}$ changes monotonically as $-6.772 \rightarrow -4.12 \rightarrow -3.64$ eV. The atomisation energy E_{at} is calculated by equation (7):

$$E_{\text{at}} = -E_{\text{ion}} - U_{\text{trans}} + E_{\text{kin}} \quad (7)$$

where E_{ion} is the energy of transformation of liquid system to the system of isolated ions (molecular dynamics measurement), U_{trans} is the energy of

transformation of isolated neutral atoms to ions with charges $\pm Z_i$, E_{kin} is the kinetic energy.

In the molecular dynamics modelling, the non-Coulomb potential is cut down at the point where the potential may differ slightly from zero. This affects the calculated atomisation energy. A small adjustment of the pair potentials (a constant) makes the calculated energy equal to the experimental value. Such adjustment in the Schommers and BELION algorithms has no effect on calculation of other properties but atomisation energy.

Experimental atomisation energy was calculated as a sum of the standard enthalpy of formation of a compound at 298 K, its heat of fusion (with opposite sign) and enthalpies of atomisation of a metal and halogen.

Atomisation energy of a system in the MD modelling was calculated for varied ionic charges to find a charge at which the atomisation energy is at maximum, and therefore, the internal energy is at minimum. The minimum of the internal energy corresponds to the minimum of the Gibbs free energy, because entropies of models with different charges are practically the same (the models' structure is the same). Therefore, this procedure defines the ionic charges at which the Gibbs free energy of a halide is at minimum and the system is at equilibrium.

3. MODELLING OF LIQUID ALKALI METALS HALIDES

Liquid LiCl at 958 K.

PPCFs for this system obtained from experimental structure factors determined in [18] are shown in Fig. 1. Non-Coulomb potentials were cut at 12.91 \AA . Lithium chloride models were constructed from 498 ions in a basic cube with a charge of lithium ion varying from 0.9 to 1.1. Good agreement was achieved between calculated and experimental PPCFs after 25 iterations of algorithm BELION. Atomisation energy and pressure of models with different lithium ion charge are given in the table below. This table also contains data for lithium and chlorine with charges equal to zero ($Z_{\text{Li}}=0$), calculated using Schommers' algorithm.

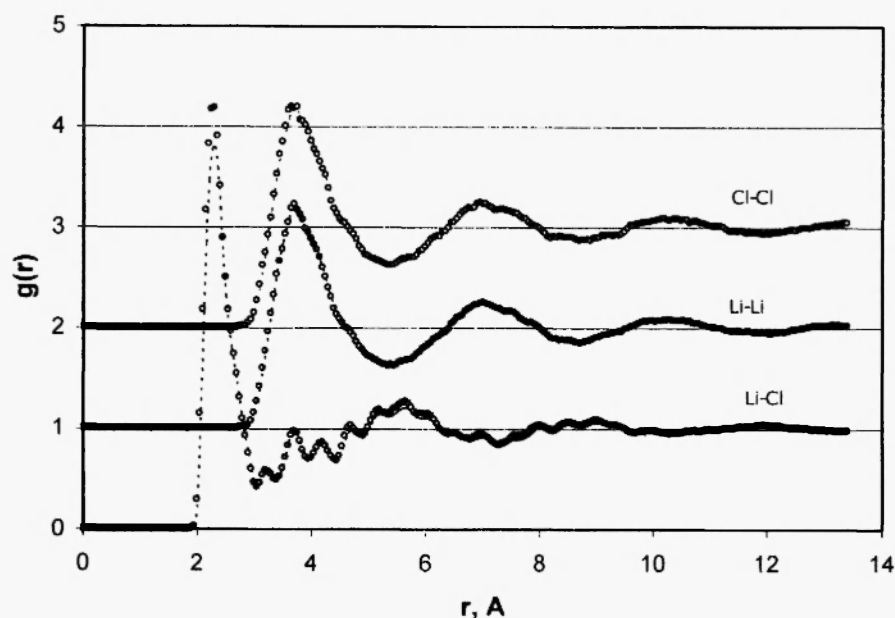


Fig. 1: Partial pair correlation functions for liquid LiCl at 958 K. Broken line: diffraction data [18]; markers: model's PPDFs. Ionic charges are ± 1.0 . Curves are shifted relatively the origin.

Z_{Li}	0	0.95	1.00	1.05	1.10
R_p	0.026	0.040	0.049	0.050	0.060
E_{at} , kJ/mol	39.7	631.3	651.4	648.6	639.3
P, GPa	1.76	1.14	1.08	1.24	1.89

Atomisation energy calculated using Schommers' method is significantly lower than an experimental value of 667.5 kJ/mole. The maximum of the atomization energy and, therefore, minimum of the internal energy are achieved at the lithium charge near +1.02. Taking into account assumptions used in calculation of ionization potentials and electron affinity, the lithium charge can be assumed equal to 1.00.

Properties of molecular dynamics model of LiCl

containing 1968 ions are given in Table 1. In this Table, U_{ij} is the energy of non-Coulomb interaction between ions i and j , U_{total} is the total potential energy which includes Coulomb energy, ionisation potential and electron affinity. The atomisation energy, which is equal to the potential energy with opposite sign (651.4 kJ/mol), is very close to the experimental value 667.5 kJ/mol. Calculated pressure is not equal to zero: however, it is very sensitive to experimental diffraction data. Shift of PPCFs by 0.05-0.10 Å can change pressure by several GPa.

The PPCFs of the model's liquid LiCl are shown in Fig. 1. They agree well with experimental data (Table 2). Discrepancy parameters for Li-Li, Cl-Cl and Li-Cl

Table 1

Properties of molecular dynamics models of liquid lithium, rubidium and caesium chlorides. N=1968.

Model	Z_M	T, K	P, GPa	Energy, kJ/mol						
				E_{kin}	U_{M-M}	U_{M-Cl}	U_{Cl-Cl}	$-U_{coul}$	U_{trans}	$-U_{total}$
LiCl	1.00	958	1.08	23.9	-3.3	81.5	-2.4	898.7	171.5	651.4
RbCl	1.10	1020	8.09	25.4	-10.2	123.2	-53.2	813.6	181.7	572.1
CsCl	1.22	968	0.30	24.1	43.8	-11.2	62.3	969.3	230.1	644.3

Table 2
Structural characteristics of molecular dynamics models of liquid alkali halides

Model	Pair	Distance, Å		Coordination number		R_g	ρ_i
		Model	Experiment	Model	Experiment		
LiCl	Li-Li	3.70	3.7 /18/	15.8 ± 1.5	-	0.049	1.09
	Li-Cl	2.28	2.3	3.4 ± 0.7	3.5 - 4.0		
	Cl-Cl	3.73	3.7	15.7 ± 1.5	-		
NaCl /10/	Na-Na	3.87	3.9 /20/	14.2 ± 1.3	13.0 /20/	0.055	1.05
	Na-Cl	2.70	2.8	4.9 ± 0.8	4.8		
	Cl-Cl	4.06	3.9	15.2 ± 1.4	13.3		
RbCl	Rb-Rb	4.80	4.9 /21,22/	15.0 ± 1.2	16.7 /21,22/	0.122	1.10
	Rb-Cl	3.22	3.2	6.4 ± 0.9	7.4		
	Cl-Cl	4.80	4.8	15.6 ± 1.2	17.1		
CsCl	Cs-Cs	4.98	4.9-4.95 /21,22/	15.7 ± 1.5	15.4 /22/	0.044	1.10
	Cs-Cl	3.28	3.4	5.5 ± 0.8	5.8		
	Cl-Cl	4.79	4.85-4.9	16.6 ± 1.5	16.3		

pairs for the model are even a little smaller than for PPCFs obtained by the Reverse Monte-Carlo method. Coordination number for the Li-Cl pair, equal to 3.4 ± 0.7 shows that liquid LiCl has a structure close to tetrahedral; a fraction of lithium ions with the Li-Cl coordination number four is 0.4. This can be attributed to the small size of lithium cation relatively chlorine anion.

The packing density of a disordered system can be characterised by the topological parameters ρ , which is defined by equation (8):

$$\rho = \sum X_i X_j r_i(ij) / (V/N)^{1/3} \quad (8)$$

where X_i is a fraction of ion i , $r_i(ij)$ is the coordinate of the first peak of the PPCF, and N is number of particles in volume V . The sum is taken over all ion pairs. Densely packed systems have $\rho = 1.08 \pm 0.02$ /19/. For LiCl $\rho = 1.09$, which means that this chloride has a dense structure.

Non-Coulomb pair potentials are presented in Fig. 2. Li-Li and Cl-Cl pair potentials are practically the same. They have a shape of the Born-Mayer potential. Li-Cl potential has an intermediate maximum near 5.5 Å. The potentials are quite shallow and become negligibly

small at the distance above 10 Å. Because of this, the molecular dynamics model of lithium chloride can be constructed with only approximately 500 ions in the basic cube.

Liquid NaCl at 1148 K.

Results of modelling of liquid NaCl at 1148 K with Schommers (2996 ions in the basic cube) and BELION (498 ions) algorithms were published in /10/, using diffraction data obtained in /20/. Ionic charges in this chloride were taken ± 1.00 . Atomisation energy calculated using algorithm BELION, 578.3 kJ/mol, is close to the experimental value 594.3 kJ/mol.

Liquid RbCl at 1020 K.

The structure of liquid RbCl was studied in /21,22/. Experimental diffraction data obtained in these works were related to 1020 K. At this temperature, RbCl density is 2.088 g/cm³ /23/, therefore, the molar volume is 57.91 cm³/mol. The length of the basic cube edge, calculated from the chloride density is 28.823 Å for $N = 498$ and 45.568 Å for $N = 1968$.

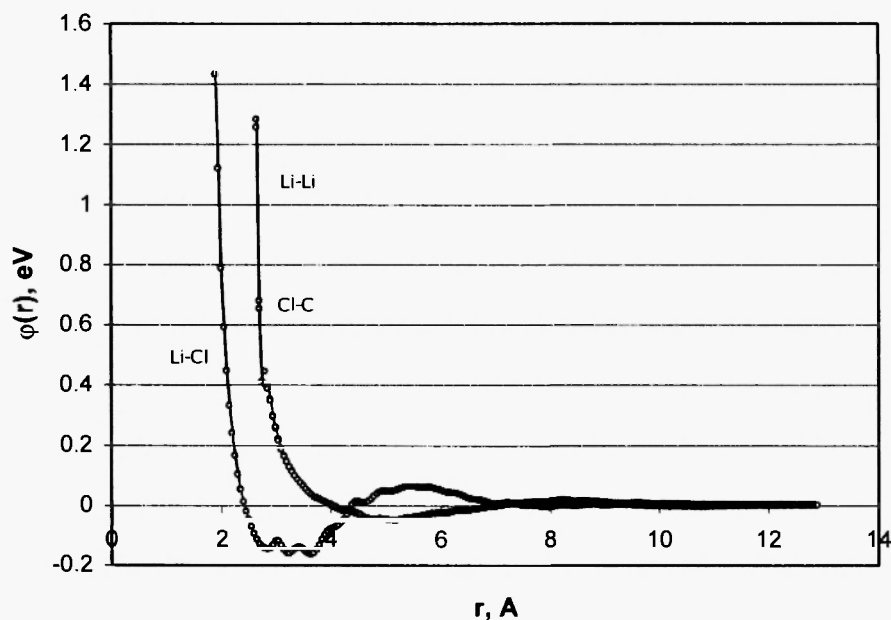


Fig. 2: Non-Coulomb potentials for liquid LiCl at 958 K. Ionic charges are ± 1.0 .

Experimental diffraction data were tested using the RMC method. The model contained 1968 ions in the basic cube. The discrepancy parameters were quite high - 0.088, 0.131 and 0.064 for Rb-Rb, Rb-Cl and Cl-Cl pairs correspondingly, which indicates that experimental PPCFs were not accurate enough.

Discrepancy parameters for the molecular dynamic models constructed using algorithm BELION were even higher. Atomisation energy and pressure of models with varying ionic charges are given below:

Z_{Rb}	0 ¹⁾	1.00	1.10	1.20
E_{at} , kJ/mol	1.0	553.3	572.1	513.8
P, GPa	3.13	5.49	8.09	7.70

¹⁾Calculated using Schommers' algorithm

Maximal atomisation energy and, therefore, minimal internal energy correspond to $Z_{\text{Rb}} \cong 1.10$. Therefore, ionic charges in liquid RbCl are ± 1.10

Properties of liquid RbCl model with 498 ions for $Z_{\text{Rb}} = 1.10$ are given in Table 2. Calculated atomisation energy 572.1 kJ/mol is 6.5% lower than the experimental value 612.0 kJ/mol. However, the calculated pressure 8.09 GPa is quite high, which means

that ions in the model are of a larger size than real ions.

The models' PPCFs depart from experimental data for first peaks of Rb-Rb and Rb-Cl pairs. Coordination number Rb-Cl is 6.4 ± 0.9 , which means that the liquid RbCl has an octahedral structure (Rb cation and Cl anion are close in size). Topological parameter $\rho_1 = 1.10$ shows that the RbCl structure is quite dense.

Non-Coulomb potentials for the RbCl system have deeper minimums and higher maximums than for the LiCl system.

Liquid CsCl at 968 K.

The structure of liquid CsCl was studied in /21/ at 968 K. Molar volume of liquid CsCl at the melting temperature (918 K) is 60.31 cm³/mol /24/, and 60.51 cm³/mol at 968 K. The calculated edge of the basic cube is 29.248 Å for 498 ions in the basic cube and 46.241 Å for 1968 ions.

Liquid RbBr at 960 K. Results of MD modelling of this system with the algorithm BELION were published in /13,14/. Experimental PPCF's of molten RbBr used in modelling were taken from works /25,26/.

MD models with varying ionic charge were constructed using the BELION algorithm for 498 ions. The potentials were cut at 13.51 Å. Atomisation energies and pressures for models with different ionic charge are given below.

Z_{Cs}	0 ¹⁾	1.10	1.15	1.20	1.25	1.30
E_{at} , kJ/mol	35.1	653.6	677.8	699.7	697.7	694.2
P, GPa	1.72	0.00	0.04	-0.20	0.35	0.30

¹⁾Calculated using Schommers' algorithm

Maximum of the atomisation energy (minimum of the internal energy) corresponds to $Z_{Cs} \equiv 1.22$. Therefore, the ionic charges in liquid CsCl are ± 1.22 .

A MD model of liquid CsCl with ionic charges ± 1.22 was also constructed with 1968 ions in the basic cube. Potentials were cut at 13.51 Å. Results of calculation of thermodynamic properties are given in Table 1. Calculated atomisation energy, 644.3 kJ/mol, is in reasonable agreement with experimental value 619.5 kJ/mol. Pressure is close to zero.

The models' PPCFs agree well with diffraction data apart from heights of Cs-Cs and Cl-Cl peaks. Liquid CsCl has a dense structure, topological parameter $\rho_1 = 1.10$.

Non-Coulomb potentials have no anomalies; their shape resembles potentials for liquid LiCl.

Ionic charges in liquid RbBr were found ± 1.00 . Calculated atomisation energy, 580.5 kJ/mol, is close to the experimental value, 564.3 kJ/mol. The difference between them is only 2.9%.

Non-Coulomb potentials for Rb-Rb and Br-Br pairs are relatively small at real distances between these ions in liquid RbBr, 0.1 eV and less. Therefore, Rb-Rb and Br-Br coordinations are governed by the Coulomb repulsion. Calculated potentials differ from Born-Mayer-Huggins potentials obtained with Fumi-Tosi parameters.

4. MODELLING OF LIQUID ALKALINE-EARTH METAL HALIDES

The structures of molten chlorides of alkaline-earth metals $MgCl_2$, $CaCl_2$, $SrCl_2$, and $BaCl_2$, have a lot in common /27,28/. Cation-anion distances can be assessed

as a sum of ionic radii. Cation-cation (M-M) and anion-anion (Cl-Cl) distances are close to those in the crystal. Coordination M-Cl number shows a trend of increasing with increasing number of metal in the periodic table: 4.3, 5.3, 6.9 and 6.4 in $MgCl_2$, $CaCl_2$, $SrCl_2$, and $BaCl_2$ correspondingly /28/. Interaction between ions in $SrCl_2$ and $BaCl_2$ can be described by the Born-Mayer potentials, which are used for pure ionic bonds. In application to $MgCl_2$ and $CaCl_2$, which have cations of a smaller size than Sr and Ba, these potentials are not good enough. In these cases, polarisation and other contributions to the potential should be taken into account /28, 29/.

MD modelling of halides of alkaline-earth metals with algorithm BELION was done in a similar way to the modelling of alkali halides, presented in the previous section. In all cases, the non-Coulomb potential was cut at 9.51 Å. Some results of this modelling were published in /30,31/.

Liquid $MgCl_2$ at 998 K.

PPCFs obtained in /27/ at 998 K are shown in Fig. 3. Interestingly, Mg-Mg and Cl-Cl distances are quite close - 3.81 и 3.56 Å correspondingly, although Coulomb repulsion between magnesium cations with a charge +2 is much stronger than between chlorine anions with a charge -1.

Calculated atomisation energy for liquid $MgCl_2$ with varying ionic charge in the MD model with 747 ions is given below:

Z_{Mg}	1.9	2.0	2.1	2.2
E_{at} , kJ/mol	961.0	977.3	979.2	930.4

The atomisation energy has a maximum at the magnesium charge near 2.05. Keeping in mind approximation in calculation of ionisation potential and electron affinity, the charge for magnesium is assumed to be equal +2.00 and the chlorine charge -1.00.

Thermodynamic characteristics of the MD model of liquid $MgCl_2$ with $Z_{Mg} = +2$ and $Z_{Cl} = -1$ with 1968 ions in the basic cube are presented in Table 3. The calculated atomisation energy, 993.8 kJ/mol is practically equal to the experimental value 988.2 kJ/mol. However, the pressure is quite high.

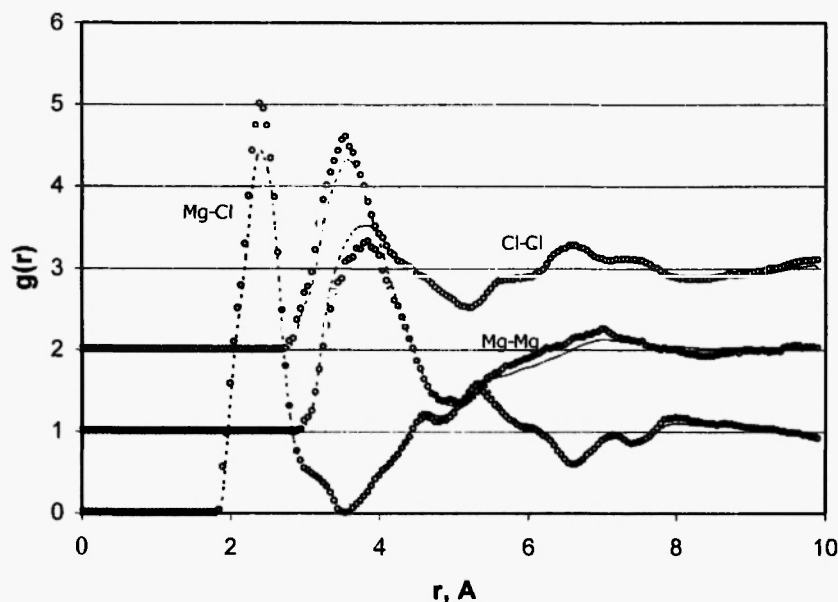


Fig. 3: Partial pair correlation functions for liquid MgCl_2 at 998 K. Broken line: diffraction data /27/; markers: model's PPCFs. Ionic charges are +2.0 and -1.0. Curves are shifted relatively the origin.

Table 3

Properties of molecular dynamics models of liquid Mg, Sr and Ba chlorides. $N=1968$.

Chloride (MCl_2)	T, K	Z_M	P, GPa	Energy, kJ/mol						
				E_{kin}	$U_{\text{M-M}}$	$U_{\text{M-Cl}}$	$U_{\text{Cl-Cl}}$	$-U_{\text{Coul}}$	U_{trans}	$-U_{\text{total}}$
MgCl_2	998	2.0	-2.9	37.3	208.6	7.9	-161.0	2540.3	1491.0	993.8
SrCl_2	1198	2.1	2.16	44.9	205.5	-182.2	91.4	2437.5	1105.8	1217.0
BaCl_2	1298	2.1	-1.2	48.6	-89.5	135.6	13.0	2330.0	938.3	1332.5

The model's PPCFs of liquid MgCl_2 are shown in Fig. 3. In general, they agree well with diffraction PPCFs. Some difference is observed in the height of PPCF's peaks for the Mg-Cl and Cl-Cl pair. It should be mentioned that the discrepancy parameters for the PPCFs constructed by the MD modelling using the algorithm BELION cannot be smaller than for PPCFs obtained by the RMC method, and RMC discrepancies are rather high for data presented in /27/.

The topological parameter $\rho_1 = 0.974$ (Table 4) indicates that liquid MgCl_2 has a densely packed

structure. Coordination number for the Mg-Cl pair is 5.2 ± 0.9 .

Non-Coulomb pair potentials are shown in Fig. 4. Mg-Cl potential has a deep minimum near 3.55 Å which originates from the deep minimum in the PPCF for the Mg-Cl pair. Possibly, this minimum is a result of experimental error in measurement of structural properties of this system. Remarkably, the Mg-Mg potential has a sharp -1.62 eV minimum at 2.95 Å and 0.95 eV maximum at 5.05 Å. Namely this minimum can be responsible for a small distance, 3.81 Å, between Mg

Table 4
Structural characteristics of molecular dynamics models of liquid halides of alkaline-earth metals.

Model	Pair	Distance, Å		Coordination number		R_g	ρ_l
		Model	Experiment	Model	Experiment		
MgCl_2	Mg-Mg	3.81	3.81 ± 0.05 /27/	5.3 ± 1.2	5 ± 1 /27/	0.102	0.974
	Mg-Cl	2.40	2.42 ± 0.03	5.2 ± 0.9	4.3 ± 0.3		
	Cl-Cl	3.57	3.56 ± 0.04	11.8 ± 1.8	12 ± 1		
CaCl_2	Ca-Ca	3.50	3.6 ± 0.1 /32/	3.7 ± 1.0	4.2 ± 0.5 /32/	0.079	1.033
	Ca-Cl	2.70	2.78 ± 0.03	5.5 ± 0.8	5.4 ± 0.3		
	Cl-Cl	3.56	3.73 ± 0.03	9.7 ± 1.3	7.8 ± 0.3		
SrCl_2	Sr-Sr	5.14	4.95 /33/	14.1 ± 2.2	13.6 /33/	0.046	1.12
	Sr-Cl	2.89	2.9	7.2 ± 1.2	6.9		
	Cl-Cl	3.88	3.80	9.6 ± 2.2	9.3		
BaCl_2	Ba-Ba	4.84	4.9 /35/	16.8 ± 1.8	14 ± 2 /35/	0.035	1.093
	Ba-Cl	3.07	3.1	6.8 ± 1.0	6.4 ± 0.2		
	Cl-Cl	3.90	3.9	10.0 ± 1.6	7 ± 1		

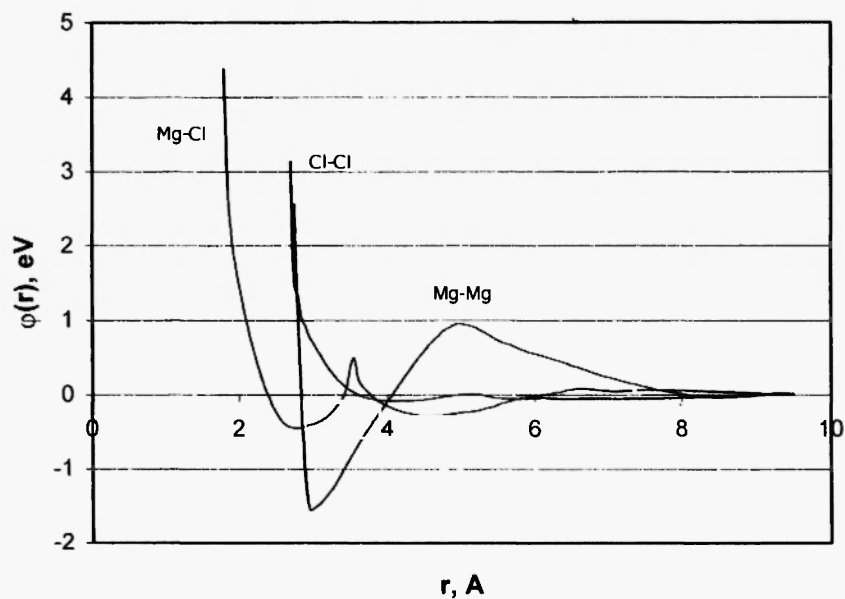


Fig. 4: Non-Coulomb potentials for liquid MgCl_2 at 998 K. Ionic charges are +2.0 and -1.0.

cations (see Fig. 3). However, this unusual shape of the Mg-Mg potential requires further examination. Pair potentials are negligibly small at distances 10 Å and above; this makes MD modelling of chloride with relatively small number of ions reliable.

Liquid CaCl_2 at 1093 K.

PPCFs for liquid CaCl_2 at 1093 K were obtained in /32/. The first PPCF's peak for Ca-Ca is located at a shorter distance (3.6 Å) than the Cl-Cl peak (3.73 Å), although magnesium cations experience much stronger Coulomb repulsion than chlorine anions (see also the MgCl_2 system). However, experimental structural factors for Ca-Cl and Ca-Ca pair are not accurate. The discrepancy parameters calculated in the RMC modelling for Ca-Ca, Ca-Cl and Cl-Cl PPCFs are equal to 0.081, 0.063 and 0.091 (at the distance up to 9.51 Å). This means that experimental data cannot be reproduced accurately in the modelling.

Indeed, in the MD modelling with the algorithm BELION (747 ions), the discrepancy parameter for the Ca-Ca and Ca-Cl PPCFs was 0.10 - 0.12, and for the Cl-Cl pair it was 0.06 (average $R_g \approx 0.10$, Table 4). Atomisation energies and pressures of MD models for CaCl_2 with varying ionic charge are given below:

Z_{Ca}	1.9	2.0	2.1
E_{at} , kJ/mol	638.1	711.9	700.1
P, GPa	20.4	18.2	18.5

The calculated atomisation energy for CaCl_2 has a maximum for $Z_{\text{Ca}} = +2.04$; however its value is significantly smaller than experimental energy 1184 kJ/mol. The pressure is very high, which resulted in compressing of models. Poor results can be attributed to inaccurate diffraction data used in the modelling.

Liquid SrCl_2 at 1198 K.

Diffraction data for liquid SrCl_2 were obtained in /33/ at 1198 K. Density of liquid chloride at this temperature is 2.697 g/cm³ /34/, molar volume 58.78 cm³/mol. This gives the edge of the basic cube with 747 ions equal to 28.966 Å, with 1968 ions - 40.006 Å.

Atomisation energy of SrCl_2 with varying ionic charge calculated by the MD modelling with the algorithm BELION (747 ions) is given below:

Z_{Sr}	1.8	1.9	2.0	2.1	2.2	2.3
E_{at} , kJ/mol	1199.1	1220.4	1225.5	1252.5	1186.7	1151.9

Maximum atomisation energy corresponds to $Z_{\text{Sr}} \approx 2.08$. Therefore, the charge of strontium cation is +2.08, and the charge of chlorine anion is -1.04. In other words, ionic charges are close to the standard values. Results of modelling are presented in Table 3. Calculated atomisation energy is very close to the experimental value 1219 kJ/mol. Pressure is quite low.

The model's PPCFs ($N = 1968$, $Z_{\text{Sr}} = 2.1$) agree well with experimental data /33/ apart from first peaks of PPCFs for Sr-Sr and Sr-Cl. Discrepancy parameters are relatively small (Table. 4). Good agreement between calculated and experimental data was also obtained for coordination numbers of all pairs. The structure of liquid SrCl_2 is dense ($\rho_1 \approx 1.12$).

Non-Coulomb potentials are of "normal" appearance without anomalies.

Liquid BaCl_2 at 1298 K.

The structure of liquid BaCl_2 was studied in /35/ at 1298 K. Density of liquid chloride at this temperature is 3.131 g/cm³ /34/, molar volume 66.508 cm³/mol, the edge of the basic cube is 30.184 Å for the cube with 747 ions and 41.688 Å for the cube with 1968.

Analysis of diffraction data obtained in /35/ by the RMC modelling shows the high accuracy of experimental data. Discrepancy parameters were 0.034, 0.033 and 0.027 for Ba-Ba, Ba-Cl and Cl-Cl PPCFs correspondingly.

MD models containing 747 ions constructed with the algorithm BELION have the following atomisation energy for varying ionic charges:

Z_{Ba}	2.0	2.1	2.2	2.3
E_{at} , kJ/mol	1292.9	1325.3	1308.8	1281.5

Barium and chlorine charges determined from the maximum of the atomisation energy are $+2.12$ и -1.06 . Properties of the MD model of liquid BaCl_2 with $Z_{\text{Ba}}=+2.1$ and $Z_{\text{Cl}}=-1.05$ containing 1968 ions are presented in Table 3. Calculated atomisation energy agrees well with the experimental value 1278 kJ/mol (the difference is 4.2%). Pressure in the system is small.

The model's PPCFs are in good agreement with experimental data. Structural characteristics of the MD model of liquid BaCl_2 are presented in Table 4. BaCl_2 has a dense structure ($\rho_1 = 1.093$).

Non-Coulomb potentials have no anomalies. Potentials and structure of BaCl_2 are close with those for SrCl_2 .

5. MODELLING OF LIQUID NOBLE METAL HALIDES

Liquid CuCl at 773 K.

MD models of liquid CuCl with algorithm BELION were constructed at 773 K using diffraction data obtained in [36, 37]. Density of CuCl is $0.0448 \text{ at } \text{\AA}^{-3}$ [37]. The edge of the basic cube of the model with 498 ions is 22.318 \AA . Atomisation energies of MD models of CuCl with varying ionic charge at 773 K are given below (non-Coulomb potential was cut off at 9.51 \AA):

Z_{Cu}	1.00	1.15	1.20	1.263	1.40
E_{at} , kJ/mol	496.8	516.0	536.3	534.8	514.5

Copper and chlorine charges at which atomisation energy is at maximum are ± 1.20 . Properties of the CuCl model are presented in Table 5 and Table 6. Calculated atomisation energy, 536.3 kJ/mol is practically equal to the experimental value 538.1 kJ/mol.

The model's PPCFs in comparison with experimental data [37] are shown in Fig. 5: non-Coulomb pair potentials are presented in Fig. 6. Model and diffraction data are in a reasonable agreement.

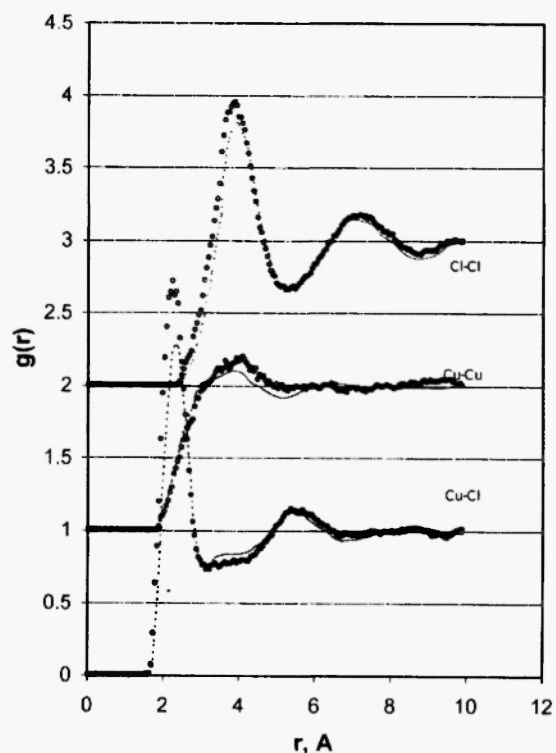


Fig. 5: Partial pair correlation functions for liquid CuCl at 773 K. Broken line: diffraction data [37]; markers: model's PPCFs. Ionic charges are ± 1.20 . Curves are shifted relatively the origin.

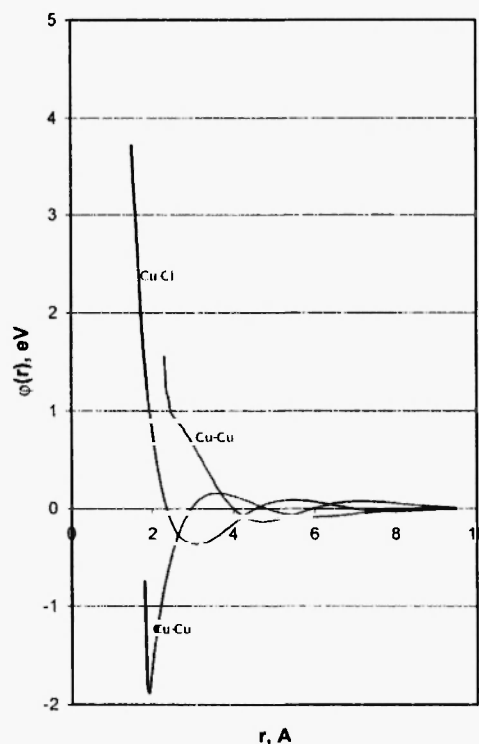


Fig. 6: Non-Coulomb potentials for liquid CuCl at 773 K. Ionic charges are ± 1.20 .

Liquid CuBr at 810 K.

Results of MD modelling of this system with the algorithm BELION using diffraction data from [26, 38] were published in [10,13,14]. Maximum of atomisation energy and, therefore, minimum of internal energy correspond to the ionic charges ± 1.48 . The model's properties calculated for liquid CuBr with these charges are given in Tables 5 and 6. Calculated atomisation energy, 488.8 kJ/mol, is smaller by experimental value, 511.4 kJ/mol, although the difference between them is not high, 4.4%.

Liquid CuI at 940 K.

Diffraction data for this system are presented on the web site of Prof. Y. Waseda's laboratory [26]. These data were used in the MD modelling with the algorithm BELION at 940 K. Models contained 498 ions in the

basic cube with edge 26.041 Å, calculated from the salt's density, 5.21 g/cm³. Atomisation energy of CuI with varying ionic charges is given below:

Z_{Ag}	1.00	1.25	1.367	1.50
E_{at} , kJ/mol	374.1	423.0	449.0	378.9

The ionic charges at which the atomisation energy is at maximum are ± 1.367 . Calculated energy, 449 kJ/mol, is close to the experimental value, 468.5 kJ/mol. Properties of liquid CuI calculated for these ionic charges are given in Table 5.

The model's structural properties are presented in Table 6. Discrepancy parameters are quite high. Non-Coulomb potential for Cu-Cu pair has deep 2.3 eV minimum at 2.36 Å. Such minimum is also observed for the Cu-Cu potential in CuCl and CuBr. Cu-Cl and Cl-Cl pairs' non-Coulomb potentials are without anomalies.

Table 5
Properties of molecular dynamics models of liquid halides of copper and silver.

Halide	T, K	Z_M	P, GPa	Energy, kJ/mol						
				E_{kin}	U_{M-M}	U_{M-Mc}	U_{Me-Me}	$-U_{\text{coul}}$	U_{trans}	$-U_{\text{total}}$
CuCl	773	1.20	-1.32	19.28	-72.3	-16.6	138.7	1291.8	705.6	536.3
CuBr	810	1.48	1.81	20.2	26.2	-140.3	191.4	1850.4	1284.2	488.8
CuI	940	1.37	-0.75	23.44	11.2	100.3	-204.2	1416.4	1060.2	449.0
AgBr	753	1.15	-1.42	18.78	-104.0	177.4	-64.0	1073.8	609.8	454.5

Table 6
Structural characteristics of molecular dynamics models of liquid copper and silver halides

Model	Pair	Distance, Å		Coordination number	R _g	ρ ₁
		Model	Experiment	Model		
CuCl	Cu-Cu	3.91	3.85 /36,37/	-	0.081	1.09
	Cu-Cl	2.24	2.32	3.8		
	Cl-Cl	3.85	3.90	12.6		
CuBr	Cu-Cu	4.44	3.05 /26,38/	-	0.096	1.07
	Cu-Br	2.29	2.38	3.6		
	Br-Br	3.83	3.88	10.8		
CuI	Cu-Cu	2.71	2.67 /26/	-	0.099	0.92
	Cu-I	2.55	2.57	3.4		
	I-I	4.49	4.37	10.4		
AgBr	Ag-Ag	3.43	3.43 /26,39/	17.3	0.079	1.04
	Ag-Br	2.69	2.70	4.5		
	Br-Br	4.08	3.97	12.6		

Liquid AgBr at 753 K.

MD models were constructed using diffraction data obtained at 753 K in [39]. Density of liquid AgBr is $0.0355 \text{ at}/\text{\AA}^3$ [39]; the edge of the basic cube with 747 ions was 24.118 \AA . Atomisation energy calculated for liquid AgBr with varying ionic charges is given below:

Z_{Ag}	1.0	1.10	1.13	1.15	1.17	1.20
E_{at} , kJ/mol	424.0	416.5	433.7	454.5	434.3	428.8

Maximum atomisation energy corresponds to silver and bromine ionic charges ± 1.15 . Calculated atomisation energy for AgBr with $Z = \pm 1.15$ (454.5 kJ/mol) is, practically, equal to the experimental value 455.3 kJ/mol. The model's thermodynamic and structural properties of liquid AgBr are presented in Tables 5 and 6 respectively.

The model's and experimental PPCFs are in good agreement. Modelling even reproduces splitting of the Ag-Ag peak to three sub-peaks. Non-Coulomb pair potentials have shallow minimums (less than 0.2 eV).

6. DISCUSSION

Experimental data on the structure of liquid chlorides were analysed by Enderby and Barnes [28, 40]. They pointed out that the structure of liquid alkali halides is well described by potentials with Fumi-Tosi parameters, and PPCFs for M-M and Cl-Cl pairs are similar despite of big difference of ion sizes. In the case of alkali-earth halides, the Born-Mayer-Huggins potentials give good results only for halides with cations of large size (Sr and Ba). In application to MgCl_2 and NiCl_2 it is necessary to take into account covalent bonds to explain very short distances between metal ions.

The results of our work show that diffraction data for liquid LiCl and CsCl are of high accuracy, but not for NaCl. This is reflected in calculation of self-diffusion coefficients in liquid NaCl: calculated coefficients with the use of experimental PPCFs are low in comparison with experiments [10]. Diffraction PPCFs for RbCl are inappropriate for MD modelling with the algorithm BELION. Their reproduction by the RMC modelling is also inadequate.

Traditionally, ionic charges in molten alkali halides were ± 1 . This paper shows that ionic charges in liquid LiCl and NaCl indeed are equal ± 1 . However, ionic charges tend to increase with increasing atomic number of the alkali metal: ± 1.10 for RbCl (tentatively), and ± 1.22 for CsCl. This can be related to the fact that the difference between the second and first ionization potentials decreases with increasing atomic number; it is equal to 70.23 eV for Li and 21.21 eV for Cs. This eases the charge transfer from a cation to an anion, which is stimulated by the Coulomb interaction.

MD modelling of liquid alkali chlorides with the algorithm BELION gives good results for atomisation energy. Calculated atomisation energies using the Schommers' algorithm are much lower than experimental values (by an order of magnitude), because this algorithm does not include long-distance Coulomb interactions.

All alkali chlorides have a dense-packed structure. Coordination number increases from Li to Cs; it depends on the cation to anion size ratio.

Non-Coulomb potentials have a similar shape for all alkali chlorides, which differ from the Born-Mayer potential. In all cases, M-M potential is close to the Cl-Cl potential. The Cl-Cl potential in different chlorides is of the same shape but different magnitude; it cannot be replaced by a single Cl-Cl potential.

It should be noted that the pair potentials established for liquid chlorides are not applicable for crystal chlorides in the calculation of crystal stability.

Enderby [40] analysing structure of MCl_2 chlorides came to a conclusion that an approximation of a simple ionic bond model is applicable only to strontium and barium chlorides, which have cations of large size, but is not appropriate for chlorides with smaller cations. Small-size cations form stable complexes of the ZnCl_4^{2-} type with a close distance between cations. Such a structure cannot be reproduced with the Born-Mayer-Huggins potentials in the ionic model, and necessitates introduction of covalent bonds [40].

These salts can be modelled using the BELION algorithm under provision of having reliable diffraction data. Such data were obtained for SrCl_2 и BaCl_2 , and are not available for CaCl_2 . Accuracy of diffraction PPCFs for MgCl_2 is also not high.

Similar to chlorides of alkali metals, the ionic

charges in chlorides of alkaline-earth metals increase with increasing cation number in the Periodic Table (from +2.00 for Mg to 2.12 for Ba). The reason is the same: decreasing difference between, in this case, the third and second ionization potentials (63.17 eV for Mg and 27.0 for Ba).

For chlorides of alkali and alkaline-earth metals, ionic charges are close to expected values of ± 1 for MCl and +2 and -1 for MCl_2 . Charges of copper and silver in halides are visibly larger than the "standard" charge of +1 [10,13,14]. This is a consequence of a relatively small difference between the second and first ionization potentials, which is 12.57 eV for Cu and 13.91 eV for Ag.

Ionic (Pauling) radii of Na, Rb, Cu, Ag, Cl, Br and I are equal to 0.95, 1.48, 0.96, 1.26, 1.81, 1.95 и 2.16 Å correspondingly. This means that the Na-Cl and Rb-Br distances in molten salts are less than the sum of ionic radii only by 0.05 и 0.09 Å. For CuCl, CuBr and CuI this difference is 0.53, 0.62 and 0.57 Å respectively, which supports the finding of this work that the copper charge in halides is above one, and that an approximation of pure ionic bond is not valid. The Ag - Br distance is less of the sum of the ionic radii by 0.52 Å, which also agrees with enhanced ionic charges. The bonds in these systems are ionic-covalent; this is reflected in a relatively low metal-halogen coordination number (Table 6).

Non-Coulomb potentials include covalent and other interactions between ions. Deep minima are seen only in Cu-Cu non-Coulomb potentials. These minima are responsible for broad first peaks of PPCFs for Cu-Cu pair in CuCl and CuBr. The Cu-Cu potential, as other pair potentials for alike ions, depends on the system.

7. CONCLUSION

Molecular dynamics modelling with the algorithm BELION gives good results for structure and internal energy of liquid halides, which agree well with experimental data. The modelling requires reliable diffraction data. The accuracy of these data may be assessed using the Reverse Monte-Carlo method. Non-Coulomb potential determined by the BELION interactions includes covalent and other non-Coulomb

interactions in the system. These interactions in addition to Coulomb potential are responsible for the liquid's structure. This is an efficient method for interpretation of experimental diffraction data and calculation of properties of liquid salts.

REFERENCES

1. Y. Waseda, *The Structure of Non - Crystalline Materials. Liquids and Amorphous Solids*. McGraw-Hill, New York, 1980.
2. L.V. Woodcock, in: *Advances in Molten Salt Chemistry*, New York, Plenum Press, **1**, 1-74 (1971).
3. F.G Fumi and M.P. Tosi, *J. Phys. Chem. Solids*, **25**, 31-43; 45-52 (1964).
4. K. Omote and Y. Waseda, *J. Phys. Soc. Japan*, **66**, 1024-1028 (1997).
5. Y. Waseda, K. Omote and S. Tamaki, *High Temp. Mater. & Processes*, **16**, 109-122 (1997).
6. K. Omote, M. Saito and Y. Waseda, *J. Phys. Soc. Japan*, **66**, 3097-3101 (1997).
7. P.D. Mitev, M. Saito and Y. Waseda, in *Liquid and Amorphous Metals-II* (Abstracts), 100 (2001).
8. F. Kirchhof, J.M. Holender and M.J. Gillan, *Phys. Rev B*, **54**, 190-202 (1996).
9. S.K. Mitra, *Phil. Mag. B*, **45**, 529-548 (1982).
10. D.K. Belashchenko, *Russ. J. Phys. Chem.*, **76**, 1461-1471 (2002).
11. D.K. Belashchenko and M.P. Momchev, *Izv. Vyssh. Uchebn. Zaved. Chern. Metall.*, **7**, 72 (1992), in Russian.
12. W. Schommers, *Phys. Lett.*, **43A**, 157-158 (1973).
13. D.K. Belashchenko and O.I. Ostrovski, *Calphad*, **28**, 523-538. (2002).
14. D.K. Belashchenko and O.I. Ostrovski, *Russ J. Phys. Chem.*, **77**, 627-635 (2003).
15. D.K. Belashchenko and O.I. Ostrovski, *Russ. J. Phys. Chem.*, **77**, 1111-1117 (2003).
16. J.E. Enderby, D.N. North and P.A. Egelstaff, *Phil. Mag.*, **14**, 961-970 (1966).
17. Y. Waseda and J. Toguri, *The Structure and Properties of Oxide Melts*, Singapore, World Scientific, 1998.
18. M.A. Howe and R.L. McGreevy, *Phil. Mag. B.*, **58**, 485-495 (1988).

19. D.K. Belashchenko, *Russian Chemical Reviews*, **66**, 733-762 (1997).
20. S. Biggin and J.E. Enderby, *J. Phys. C: Solid State Phys.*, **15**, L305-L309 (1982).
21. J. Locke, S. Messori, R.J. Stewart, R.L. McGreevy and E.W.J. Mitchell, *Phil. Mag. B.*, **51**, 301-315 (1985).
22. E.W.J. Mitchell, P.F.J. Poncet and R.J. Stewart, *Phil. Mag.*, **34**, 721 (1976).
23. *Chemical Handbook* (Ed. B.P. Nikol'skij), Leningrad-Moscow, V. 1 & 2, 1962 (in Russian).
24. R.V. Gopala Rao and R. Venkatesh, *Phys. Stat. Sol. B.*, **157**, 65 (1990).
25. M. Saito, S. Kang and Y. Waseda, *Japanese J. Appl. Phys.*, Pt 1, **38** (Suppl.), 596-599 (1998).
26. Web site: www.iamp.tohoku.ac.jp/home-j.html
27. S. Biggin, M. Gay and J.E. Enderby, *J. Phys. C: Solid State Physics*, **17**, 977-985 (1984).
28. J.E. Enderby, in *Molten Salt Chemistry* (Eds. G. Mamantov, R. Marassi and D. Reidel), Publ. Comp. NATO SAD., **202**, 1-15 (1967).
29. J.E. Enderby, *J. Phys. C: Solid State Physics*, **15**, 4609-4625 (1982).
30. D.K. Belashchenko and O.I. Ostrovski, in *VII International Conference on Molten Slags Fluxes and Salts* (Abstracts), Cape Town, South Africa, 25 – 28 January 2004.
31. D.K. Belashchenko and O.I. Ostrovski, *Russ. J. Phys. Chem.*, **77**, 1972-1983 (2003).
32. S. Biggin and J.F. Enderby, *J. Phys. C: Solid State Physics*, **14**, 3577-3583 (1981).
33. R.L. McGreevy and E.W. Mitchell, *J. Phys. C: Solid State Physics*, **15**, 5537-5550 (1982).
34. *Molten Salts Handbook*, Leningrad, Chemistry, V.1, 1971 (in Russian).
35. F.G. Edwards, R.A. Howe, J.E. Enderby and D.L. Page, *J. Phys. C: Solid state physics*, **11**, 1053-1057 (1978).
36. D.L. Page and K. Mika, *J. Phys. C: Solid State Phys.*, **4**, 3034 (1971).
37. S. Eisenberg, J.-F. Jal, J. Dupuy, P. Chieux and W. Knoll, *Phil. Mag. A*, **A46**, 195-209 (1982).
38. M. Saito, C. Park, K. Omote K., K. Sugiyama and Y. Waseda, *J. Phys. Soc. Japan*, **66**, 633-640 (1997).
39. M. Saito, S. Kang, K. Sugiyama and Y. Waseda, *J. Phys. Soc. Japan.*, **68**, 1932-1938 (1999).
40. J.E. Enderby and A.C. Barnes, *Rep. Prog. Phys.*, **53**, 85-179 (1990).

